A Delay-Aware Cyber-Physical Architecture for Wide-Area Control of Power Systems

Damoon Soudbakhsh, Aranya Chakrabortty, Francisco Javier Alvarez, and Anuradha M. Annaswamy

***Abstract*— In this paper we address the problem of wide-area control of power systems in presence of different classes of network delays. We pose the control objective as an LQR minimization of the electro-mechanical states of the swing equations, and exploit flexibilities and transparencies of the communication network such as scheduling policies, bandwidth to co-design a delay-aware state feedback control law. Hence, unlike the traditional robust control designs, our design is delay-aware, not delay-tolerant. A key feature of our method is to retain the samples of the control input until a desired time instant using shapers before releasing them for actuation to *regulate* the delays entering the controller. In addition, our co-design includes an overrun management strategy to guarantee stability of the closed-loop power system model in case of occasional PMU data losses. This strategy allows dropping messages with very large delays, reducing resource utilization during busy network times, and improving overall performance of the system. We illustrate our results using a 50-bus, 14-generator, 4-area power system model, and show how the proposed arbitrated controller can guarantee significantly better closed-loop performance than traditional robust controllers.**

I. INTRODUCTION

The wide-area measurement systems (WAMS) technology using Phasor Measurement Units (PMUs) has been regarded as the key to guaranteeing stability, reliability, state estimation, control, and protection of next-generation power systems [1], [2]. However, with the exponentially increasing number of PMUs deployed in the North American grid, and the resulting explosion in data volume, the design and deployment of an efficient wide-area communication and computing infrastructure is evolving as one of the greatest challenges to the power system and IT communities. For example, according to UCAlug Open Smart Grid (OpenSG) [3], every PMU requires 600 to 1500 kbps bandwidth, 20 ms to 200 ms latency, almost 100% reliability, and a 24-hour backup. With several thousands of networked PMUs being scheduled to be installed in the United States by 2020, wide-area control systems will require a significant Gigabit per second bandwidth. The challenge is even more aggravated by the fact that utilities are unlikely to establish expensive dedicated communication links, for such system-level controls, implying that the communication infrastructure must be implemented on top of their existing subnetworks. As a result, PMU data used for control will have to be transported over a *shared* resource, sharing bandwidth with other ongoing applications, giving rise to not only transport delays, but also significant delays due to queuing and routing. Figure 1(a), for example, shows an example of a large-scale spatially distributed power network (a 50-machine Australian power system, which will be used for our simulations), consisting of four balancing regions under different utility companies, each equipped with multiple PMUs; Figure 1(b), on the other hand, shows the envisioned architecture of wide-area communication, where PMUs inside any balancing region send data to their local controllers via a common virtual private network (VPN), and to remote controllers in other regions over a multi-hop wide-area network, an example of which can be a Software Defined Network (SDN) [4]. Each area is equipped with its own dedicated VPN server which routes the incoming PMU data-streams to the respective controllers. Currently, there is very little insight on how the different protocols for PMU data transport through this network may lead to a variety of delay patterns, and how controlling these delays can potentially help wide-area control designs. Majority of the ongoing NASPI-net activities are devoted to the hardware planning aspects of the communication [5], [6]. Only a modest effort has been made so far to study the impact of delays [7], [8], with the typical approach being to design a nominal controller and testing its robustness and sensitivity to the worst-case delays.

Motivated by this challenge, in this paper we propose a novel cyber-physical WAMS architecture, where wide-area control designs can be implemented on the top of a secure distributed computing infrastructure connected by high-speed wide-area networks that are dynamically *programmable* and *reconfigurable*. Our objective is to develop a set of optimal control algorithms for damping small-signal oscillations in power and voltages following disturbances, and investigate how these controllers can be co-designed in sync with communication delays in order to make the closed-loop system resilient and *delay-aware*, rather than just *delay-tolerant*. We formulate the control objective as an LQR minimization of the electro-mechanical swing states and excitation voltages of synchronous generators through excitation control. We present an arbitration approach by which the flexibilities of the wide-area communication network (such as scheduling policies, bandwidth, etc.) can be exploited to co-design a delay-aware state feedback control law [9]–[11]. The approach is basically twofold. First, we estimate the worst-case delays in the wide-area network using a predictive network traffic model. Second, we use these estimates to design our LQR controller. This essentially means that we regulate the delays entering our controller.

This work was supported in part by the NSF Grant No. ECCS-1135815 via the CPS initiative and NSF grant ECS 1054394.

D. Soudbakhsh, F.J. Alvarez, and A.M. Annaswamy are with Massachusetts Institute of Technology, Cambridge, MA 02139, USA {damoon,alvarezf, aanna}@mit.edu

A. Chakraborty is with North Carolina State University Raleigh, NC 27695, USA achakra2@ncsu.edu

Hence, unlike the traditional robust control designs presented in the papers referenced above, our design is delay-aware, not delay-tolerant. They are, therefore, much more reliable and practical to implement. We assume PMUs to be installed at the terminal buses of all generators so that all swing states are available for feedback. An added benefit is that relatively lower network utilizations are needed to achieve this high performance. In addition, our co-design includes an overrun management system to guarantee stability of the system in case of occasional losses. Such overrun strategy allows dropping messages with very large delays, which can reduce resource utilization during busy network times.

The remainder of the paper is organized as follows. In §II, we state the problem addressed in this paper in more detail. Dynamics of the systems with delays and design of our optimal controller are presented in §IV and §IV-B, respectively. the overrun strategy is presented in §VI. We illustrate our results using a 50-bus power system model in §VII. Some concluding remarks are given in §VIII.

II. Wide Area Control Problem

Consider a power system network with q buses. Without loss of generality, classify the first n buses to be *generator buses* and the remaining $(q-n)$ buses as *load buses* meaning that active and reactive power are extracted from these buses in the form of loads. The voltage at the i^{th} bus is denoted as $\tilde{V}_i = V_i \angle \theta_i$ where V_i is the magnitude (volts) and θ_i is the phase (radians). The internal voltage phasor of a synchronous generator connected to any generator bus is denoted as $\tilde{E}_i = E_i \angle \delta_i$, $i = 1:n$. Each synchronous generator may be modeled by a set of third-order differential algebraic equations [12]

$$\dot{\delta}_i = \omega_i - \omega_s \quad (1)$$

$$2H_i \dot{\omega}_i = P_{mi} - D_i(\omega_i - \omega_s) - P_i^G \quad (2)$$

$$\tau_i \dot{E}_i = -\frac{x_{di}}{x'_{di}} E_i + \frac{x_{di} - x'_{di}}{x'_{di}} V_i \cos(\delta_i - \theta_i) + \tilde{E}_{Fi} \quad (3)$$

$$P_i^G = \frac{E_i V_i}{x'^i_d} \sin(\delta_i - \theta_i) + \left(\frac{x'_{di} - x_{qi}}{2x_{qi} x'_{di}}\right) V_i^2 \sin(2(\delta_i - \theta_i)) \quad (4)$$

$$Q_i^G = \frac{E_i V_i}{x'^i_d} \cos(\delta_i - \theta_i) - \left(\frac{x'_{di} - x_{qi}}{2x_{qi} x'_{di}} - \frac{x'_{di} - x_{qi}}{2x_{qi} x'_{di}} \cos(2(\delta_i - \theta_i))\right) V_i^2 \quad (5)$$

where, the states δ_i, ω_i and E_i are, respectively, the generator phase angle (radians), rotor velocity (rad/sec), and the quadrature-axis internal emf; ω_s is the synchronous frequency of 120π radian/sec; P_i^G and Q_i^G are, respectively, the active and reactive power produced by the i^{th} generator (MW and Mega VAr), $2H_i$ is the inertia constant (seconds), D_i is the generator damping, P_{mi} is the mechanical power input to the i^{th} turbine (MW); τ_i is the excitation time constant (seconds); x_{di}, x'_{di}, and x_{qi} are the direct-axis salient reactance, direct-axis transient reactance, and quadrature-axis salient reactance (all in ohms), respectively. The control variable is the field voltage E_{Fi}, which is the variation of $\tilde{E}_{Fi}$ from the equilibrium point. Equations (1)-(2) follow from Newton's second law of motion applied to the internal states of the i^{th} generator. The algebraic variables at any bus, however, follow Kirchoff's law manifesting in the form of

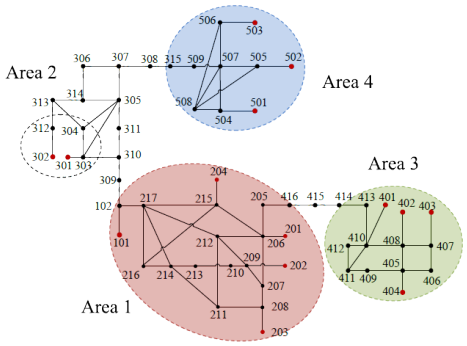

(a) Multi-Area Power System Network

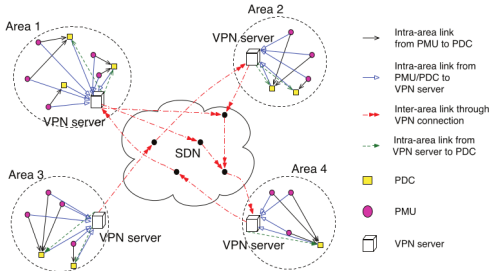

(b) Envisioned architecture for wide-area communication

Fig. 1: a) Multi-Area Power System Network, b) Envisioned architecture for wide-area communication.

active and reactive power balance

$$0 = \sum_{k \in \mathcal{N}_i} P_{ik} - P_i^G, \quad 0 = \sum_{k \in \mathcal{N}_i} Q_{ik} - Q_i^G, \quad (6)$$

$$0 = \sum_{k \in \mathcal{N}_j} P_{jk} + P_j^L, \quad 0 = \sum_{k \in \mathcal{N}_j} Q_{jk} + Q_j^L, \quad (7)$$

where $i = 1:n$, $j = n+1:q$, $\mathcal{N}_i$ denotes the set of bus numbers that are connected to bus i, i.e., the neighbor set of bus i. The dynamical model for the entire system can be constructed by relating the generator models, load models and transmission line models over any given interconnection of the n buses making use of the power balance equations (6)-(7). Considering small perturbations $(\delta_{i0}, \omega_s, E_{i0}, V_{i0}, \theta_{i0})$, $i = 1:n$, the overall linearized $(3n)^{th}$-order dynamic model of the network can be expressed as

$$\begin{bmatrix} \Delta\dot{\delta}(t) \\ 2H\Delta\dot{\omega}(t) \\ T\Delta\dot{E}(t) \end{bmatrix} = \underbrace{\begin{bmatrix} 0 & I & 0 \\ -L & -D & -P \\ K & 0 & J \end{bmatrix}}_{\mathscr{A}} \begin{bmatrix} \Delta\delta(t) \\ \Delta\omega(t) \\ \Delta E(t) \end{bmatrix} + \underbrace{\begin{bmatrix} 0 & 0 \\ I & 0 \\ 0 & I \end{bmatrix}}_{\mathscr{B}} \begin{bmatrix} \Delta P_m \\ \Delta E_F \end{bmatrix} \quad (8)$$

where $\Delta\delta = \text{col}(\Delta\delta_1, \cdots, \Delta\delta_n)$, $\Delta\omega = \text{col}(\Delta\omega_1, \cdots, \Delta\omega_n)$, $\Delta E = \text{col}(\Delta E_1, \cdots, \Delta E_n)$, $\Delta P_m = \text{col}(\Delta P_{m1}, \cdots, \Delta P_{mn})$, $\Delta E_F = \text{col}(\Delta E_{F1}, \cdots, \Delta E_{Fn})$, $H = \text{diag}(H_1, \cdots, H_n)$, and $T = \text{diag}(\tau_1, \cdots, \tau_n)$. The expressions for the various matrices on the RHS can be found in [2]. In (8), the turbine mechanical power ΔP_m typically has a much lower bandwidth than needed for oscillation damping. Therefore, for all practical wide-area control designs, ΔP_m is treated as zero, and ΔE_F is designed via PMU data feedback.

The next step is to design a controller for system (8). Using a non-singular matrix $\mathcal{T}$ representing elementary column and row transformations, we rearrange the states $(\Delta\delta, \Delta\omega, \Delta E)$ in the form of the tuple $x_i \stackrel{\text{def}}{=} (\Delta\delta_i, \Delta\omega_i, \Delta E_i)$ for every generator

i, and define $u_i = \Delta E_{F_i}$. By defining $X(t) = \text{col}(x_1, \ldots, x_n(t))$ and $U(t) = \text{col}(u_1, \ldots, u_n)$, to include all states and inputs of the syste, we write the continuous-time dynamic model of the power system as

$$\dot{X}(t) = A_c X(t) + B_c U(t), \tag{9}$$

where $A_c \in \Re^{N\times N}$ and $B_c \in \Re^{N\times M}$, are the appropriate size matrices for the vectors of all the states and inputs, with $N \stackrel{\text{def}}{=} \sum_{i=1}^{n} n_i$ and $M \stackrel{\text{def}}{=} \sum_{i=1}^{n} m_i$, and defined as

$$A_c \stackrel{\text{def}}{=} \mathcal{T}\mathcal{A}\mathcal{T}^T, \qquad B_c = \mathcal{T}\mathcal{B}. \tag{10}$$

The Wide Area control problem is to design U in (9) such that system (8) is stable.

In practice, however, the feedback controller $U(t)$ will be affected by the network delays. For the purpose of this paper, we classify these delays into three types

- Small delays if the feedback measurements are communicated from PMUs located very close to a given controller,
- Medium delays if the measurements are communicated from PMUs from distant buses but still within the operating region of the same utility company,
- Large delays if the measurements are communicated from remote buses that belong to a different utility company.

Our objective is to design a controller $U(t)$ to minimize a quadratic cost function $\mathcal{J}(X(t), U(t))$ in presence of multiple delays belonging to the three categories mentioned above. We use flexibility and transparancies of the messages as in [9], [10] to design the controller in §IV-B. The input has the form

$$U(t) = KX(t) + GU(t-\tau), \tag{11}$$

meaning that it is a linear combination of the current states and the previous inputs of the system. This approach is different from traditional robust control, where the design is independent of τ and the system relies on the robustness of the controller to τ (e.g. [13]).

The other aspect of this work is the development of an overrun analysis to guarantee stability of the system if the messages are lost. This overrun strategy consists using previously available information until a new message arrives, and aborting the computation of the message altogether if it arrives with a very large delay. The latter allows one to achieve the desired control performance while freeing up resources for other applications in the network. Tools from switching theory are used to ensure that stability is maintained even in the face of varying delays in the messages.

III. Delay Model for Wide-Area Communication

Following [14], the stochastic end-to-end delay experienced by any PMU data sample in a wide-area network consists of three components: the minimum deterministic delay denoted by m, the Internet traffic delay with Probability Density Function (PDF) denoted by ϕ_1, and router processing delay with PDF denoted by ϕ_2. Then, the PDF of the sum of three independent components is as follows:

$$\phi(t) = p\phi_2(t) + (1-p)\phi_1 * \phi_2(t), \quad t \geq 0, \tag{12}$$

with $\phi_1 * \phi_2(t) = \int_0^t \phi_2(u)\phi_1(t-u)du$. Here p is the probability of open period of the path with no Internet traffic, and the router processing delay can be well approximated by a Gaussian density function $\phi_2(t) = \frac{1}{\sigma\sqrt{2\pi}} e^{-\frac{(t-\mu)^2}{2\sigma^2}}$, where $\mu > m$. The Internet traffic delay is modeled by an alternating renewal process with exponential closure period when the Internet traffic is on, with the PDF $\phi_1(t) = \lambda e^{-\lambda t}$, where λ^{-1} models the mean length of the closure period. The benchmark value of all parameters of this model are set as: $p = 0.58, \lambda = 1.39, \mu = 5.3, \sigma = 0.078$ [14].

Equatin (12) can be rewritten as

$$\phi(t) = \frac{p}{\sigma\sqrt{2\pi}} e^{-\frac{(t-\mu)^2}{2\sigma^2}} + \frac{\lambda(1-p)}{\sigma\sqrt{2\pi}} e^{-\lambda t} \int_0^t e^{\lambda s - \frac{(s-\mu)^2}{2\sigma^2}} ds. \tag{13}$$

We calculate the integral part of (13) by using the error function $\text{erf}(x) = \frac{2}{\sqrt{\pi}} \int_0^x e^{-t^2} dt$. Then, the complete expression of the PDF is

$$\begin{aligned} \phi(t) = \quad & \frac{p}{\sigma\sqrt{2\pi}} e^{-\frac{(t-\mu)^2}{2\sigma^2}} + \frac{\lambda(1-p)}{2} e^{(\frac{1}{2}\lambda^2\sigma^2 + \mu\lambda)} \text{erf}(\frac{\lambda\sigma^2 + \mu}{\sqrt{2}\sigma}) e^{-\lambda t} \\ + \quad & \frac{\lambda(1-p)}{2} e^{(\frac{1}{2}\lambda^2\sigma^2 + \mu\lambda)} e^{-\lambda t} \text{erf}(\frac{t - \lambda\sigma^2 - \mu}{\sqrt{2}\sigma}). \end{aligned} \tag{14}$$

By using the partial integral method and the first derivative of the error function, $\frac{d}{ds}\text{erf}(s) = \frac{2}{\sqrt{\pi}} e^{-s^2}$, we derive the CDF of the delay model as follows:

$$\begin{aligned} P(t) = & \int_{-\infty}^{t} \phi(s) ds = \frac{1}{2}[\text{erf}(\frac{\mu}{\sqrt{2}\sigma}) + \text{erf}(\frac{t-\mu}{\sqrt{2}\sigma})] + \\ & \frac{(1-p)}{2} e^{(\frac{1}{2}\lambda^2\sigma^2 + \mu\lambda)} [\text{erf}(\frac{\lambda\sigma^2 + \mu}{\sqrt{2}\sigma}) + \text{erf}(\frac{t - \lambda\sigma^2 - \mu}{\sqrt{2}\sigma})]. \end{aligned} \tag{15}$$

The CDF (15) will be used to estimate the maximum delays in the wide-area network in §IV and design of τ_{th} in §VI. The wide-area network (such as SDN) is dynamically programmable and reconfigurable so that the network specifications can be designed to achieve desired delay values. Alternatively, or in addition to that, one can also modify the scheduling policy and the priority of using PMU data samples to design the delays, as illustrated in the next section.

IV. Delay-Aware Wide-Area LQR Control

In this section, we consider the PMU data communication delays and their effects on the design of closed-loop dynamics of the power system model (8). First, we investigate the effect of communication delays on the closed loop performance, and develop a model for dynamic response of the system in §IV-A, then we use this model to develop the controllers and a procedure to implement the controller.

A. Dynamic effects of delays due to shared resources

As mentioned in §II, communication delays depend on the data sharing protocols as well as the relative distance between the PMU and the excitation controller. To put the relative size of delays in perspective, we consider the measurements from the first generator $x_1(t)$, and how they

spread over the network. Such data become available for the controller located at generator 1 with a very short delay τ_{11}, whereas the same measurement may reach the controller block of the third generator with a large delay τ_{13}. If generator 3 is located in a different area than generator 1, the delay become larger (inter-area delay). Delays experienced by the measurements from generator i at the actuator of the j^{th} generator is denoted by τ_{ij} and stacking them together results in the form of the following matrix

$$\tau \stackrel{\text{def}}{=} \begin{bmatrix} \tau_{11} & \cdots & \cdots & \tau_{1n} \\ \vdots & \ddots & & \vdots \\ \tau_{i1} & & \tau_{ii} & \tau_{in} \\ \vdots & & \ddots & \vdots \\ \tau_{n1} & \cdots & \cdots & \tau_{nn} \end{bmatrix}, \tag{16}$$

We note that generator i has n_i states, and therefore it is possible to have up to n_i delays associated with its states as well. For such cases, τ_{ij} are matrices themselves. Without loss of generality, we consider a case where all elements of x_i experience the same amount of delay and τ_{ij} are scalar.

The delays in (16) can reduce efficiency of the designed system or even destabilize it. We design a controller for (9) with taking their implementation including communication delays into account; such delays can be estimated using a method such using the one presented in §III. Since the controllers are implemented using digital logic blocks, a discrete-time analysis is used. We start with (9) with a sampling interval h. In order to bring individual elements τ_{ij} of matrix τ in (16) into the control design and implementation, we break the interval h into to smaller intervals at which the inputs are updated as new measurements arrive at the controller block from locally, within each area, and from other areas (see figure 2). For example, input of the first generator $u_1[k]$ is divided to $\begin{bmatrix} u_{11}[k] & u_{12}[k] & u_{13}[k] \end{bmatrix}$, where $u_{ij}(k)$ denotes the input of the i^{th} generator adjusted using the measurements of j^{th} generator as shown in Fig. 2. Using the same logic for all generators, we derive the discrete-time model of the system as:

$$\begin{aligned} X[k+1] = \quad & AX[k] + B_{31}^1 u_{13}[sk] + B_{21}^1 u_{12}[k] + \\ & + B_{11}^1 u_{11}[k] + B_{12} u_{13}[k-1] + \\ & + \sum_{i=2}^{n} \sum_{j=1}^{m(i)} B_{j1}^i u_{ij}[k] + \sum_{i=2}^{n} B_{i2}^i u_{ik(i)}[k-1], \end{aligned} \tag{17}$$

where $m(i)$ shows the number of times that the inputs are updated in each generator (number of distinct delays) for every row of the matrix τ in (16), and $k(i)$ is the index of the largest delay in row i of (16). In (17), it is assumed that the diagonal terms have least delays in the system, but it can be easily extended to include other cases. Also, A, B_{j1}^i, and B_{i2}^i for $i = 1$ and $j = 1:3$ are defined as

$$A = e^{A_c \cdot h}, \quad B_{31}^1 = \int_0^{h-\tau_{13}} e^{A_c \cdot v} dv B_c, \quad B_{21}^1 = \int_{h-\tau_{13}}^{h-\tau_{12}} e^{A_c \cdot v} dv B_c,$$

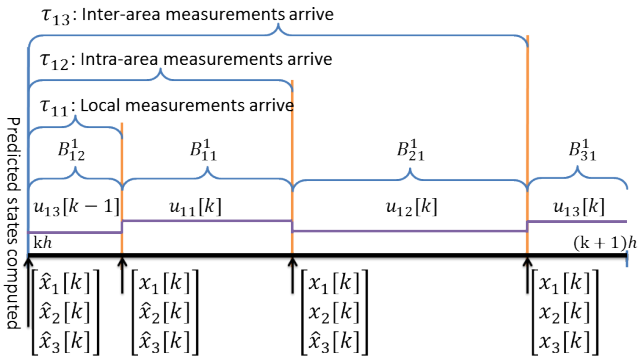

Fig. 2: Discrete time delays with τ_{11}(local delays) $<$ τ_{12}(intra-area delays) $<$ τ_{13}(inter-area delays); the vector indicated next to the arrow represents the state that is used to compute the corresponding input u_{ij}. Wherever the states are not available, they are replaced by their predicted values.

$$B_{11}^1 = \int_{h-\tau_{12}}^{h-\tau_{11}} e^{A_c \cdot v} dv B_c, \quad B_{12}^1 = \int_{h-\tau_{11}}^{h} e^{A_c \cdot v} dv B_c \tag{18}$$

Similarly, the expressions for B_{j1}^i and B_{i2}^i for any other i and j can be found. By defining new matrices B_1 and B_2 as

$$B_1 \stackrel{\text{def}}{=} \begin{bmatrix} B_{11}^1 & B_{21}^1 & B_{31}^1 & B_{11}^2 & \cdots & B_{31}^3 \end{bmatrix} \tag{19}$$

$$B_2 \stackrel{\text{def}}{=} \begin{bmatrix} 0 & 0 & B_{12}^1 & 0 & \cdots & B_{32}^3 & 0 \end{bmatrix}, \tag{20}$$

equation (17) can be written as:

$$X[k+1] = AX[k] + B_2 U[k-1] + B_1 U[k]. \tag{21}$$

By defining an augmented state $Z[k] = [X[k]^T \;\; U[k-1]^T]^T$, (21) is written as:

$$Z[k+1] = \begin{bmatrix} A & B_2 \\ 0 & 0 \end{bmatrix} Z[k] + \begin{bmatrix} B_1 \\ I \end{bmatrix} U[k], \tag{22}$$

where $I \in \Re^{M_i \times M_i}$ is an identity matrix, and $M_i \stackrel{\text{def}}{=} \sum_{i=1}^{n} m(i)$. Equation (22) shows that an excitation control law of the form

$$U[k] = K_0 X[k] + G_0 U[k-1] \tag{23}$$

stabilizes the power system (8). In other words, the proposed excitation controller needs feedback from the current state samples as well as the past input samples to stabilize the closed-loop swing dynamics with communication delays. We note that using control law of (23), closed loop dynamics of the system can be described as:

$$Z[k+1] = \begin{bmatrix} A + B_1 K_0 & B_2 + B_1 G_0 \\ K_0 & G_0 \end{bmatrix} Z[k] \stackrel{\text{def}}{=} \Gamma_n Z[k] \tag{24}$$

B. Delay-aware Control Design

As mentioned in the previous section, it is possible to rearrange the dynamic system with no delays into a controllable form; however, implementing such controllers is not efficient since some states are not available for the controller to compute the excitation voltage inputs. For example, in Fig. 2, the input $u_{11}[k]$ needs the PMU measurements of x_1, x_2, and x_3 at time kh, while x_2 and x_3 are significantly delayed and are not available to the controller at $kh + \tau_{11}$. On

the other hand, augmenting the system with states at previous instants (for example, adding $X[k-1]$ into Z) usually results in an uncontrollable plant. So, we propose designing the controller using (22) and the *predicted* values $\widehat{x}_i[k]$ for any missing state $x_i[k]$ at the computational blocks until new measurements arrive. Such an approach permits the non-zero eigenvalues of the closed loop system (in discrete-time) to remain unchanged. For example, as shown in Fig. 2, we use predicted values $\widehat{x}_2$ and $\widehat{x}_3$ along with actual measurement x_1 at $kh+\tau_{11}$. Similarly, at $kh+\tau_{12}$, instead of waiting for inter-area messages to arrive, we use actual measurements x_1 and x_2 and predicted value $\widehat{x}_3$ for the computations of the control input. Finally, at $kh+\tau_{13}$, since all the measurements arrive by $kh+\tau_{13}$, all measured states x_i rather than their predicted values $\widehat{x}_i$ are used to adjust the control input.

We can use any control strategy for this plant, and we choose the controllers to minimize the following LQR cost function

$$\min . \mathscr{J} = \frac{1}{2}\sum_{0}^{\infty} Z[k]^T Q_{ancs} Z[k] + U[k]^T R_{ancs} U[k] \qquad (25)$$

with $Q_{ancs} \succeq 0$ and $R_{ancs} \succ 0$ being semi-positive and positive definite matrices, respectively.

C. Control Implementation

As indicated in the previous section, the inputs are based on the gains that minimize cost function (25). Since, not all the PMU measurements become available at the same time, we propose using predicted values of the states $\hat{x}_i[k]$ for the short time intervals within each period until they become available (see Fig.2). So, we define a set of transformation matrices T_i such that $\mathcal{T}_i^{(1)} X$ gives the available measurements at the current time, and $\mathcal{T}_i^{(2)} X$ are the states that need to be estimated. Using T_i the closed loop dynamics of the system is represented by:

$$\begin{bmatrix} Z[k+1] \\ Z[k] \end{bmatrix} = \begin{bmatrix} A+B_1K_0\mathcal{T}^{(1)} & B_2+B_1(G_0+K_0\mathcal{T}^{(2)}B_1) & B_1K_0\mathcal{T}^{(2)}A & B_1K_0\mathcal{T}^{(2)}B_2 \\ K_0\mathcal{T}^{(1)} & G_0+K_0T_2B_1 & K_0\mathcal{T}^{(2)}A & K_0\mathcal{T}^{(2)}B_2 \\ I & 0 & 0 & 0 \\ 0 & I & 0 & 0 \end{bmatrix} \begin{bmatrix} Z[k] \\ Z[k-1] \end{bmatrix} \qquad (26)$$

where $\hat{X}[k]$ was replaced by the available values using the following relation:

$$\hat{X}[k] = AX[k-1] + B_1U[k-1] + B_2U[k-2] \qquad (27)$$

In the next section, we will show that the resulting closed-loop dynamics in (26), which is denoted as the "ANCS", results in a much better performance when compared to a design that ignores delays. The elements τ_{ij} of the delay matrix τ in (16) can be estimated using the method presented in §III. Further, one can use a shaper to regulate the delays [10].

V. Guaranteeing Optimal Dynamic Performance

In this section we present an approach to find the optimal parameters to design the LQR controller of §IV-B based on minimizing (25). $\mathscr{J}$ consists of two weighting functions on states Q_{ancs} and inputs of the system R_{ancs}. Section V-A presents tuning parameters for Q_{ancs} and §V-B presents different components of the weights and how they affect the closed-loop dynamic performance of the power system (8).

A. Optimizing State Cost Q_{ancs}

To better describe the state cost, we consider it in the following form

$$Q_{ancs} = \begin{bmatrix} Q_{lqr} & 0 \\ 0 & R_{ancs} \end{bmatrix}, \qquad (28)$$

$Q_{lqr} \succeq 0$ should be chosen to achieve the following:

1) Minimize $\Delta\omega(t)$ which is the deviation of the rotor velocities from the synchronous speed,
2) Minimize ΔE: deviations of the quadrature-axis internal emf from their nominal values.
3) Minimize deviations of the active power inside each area to achieve minimum deviation of the phase difference $(\Delta\delta_i - \Delta\delta_j)$, for any two generators i and j in the same area.

So we choose $X^T Q_{lqr} X$ as following:

$$X^T Q_{lqr} X = \sum_{i=1}^{P}\sum_{j=1}^{p_i} \alpha_{ij}(\Delta\delta_i - \Delta\delta_j)^2 + \sum_{j=1}^{n} (\beta_j \Delta\omega_i^2 + \gamma_j \Delta E^2), \quad (29)$$

where α_{ij}, β_j, and γ_j are normalized weight coefficients, whose values depend on which states need to be penalized more than others for a given design problem.

While choosing Q_{ancs} follows almost the same procedure as for the nominal mode (i.e. LQR with zero delay), choosing matrix R_{ancs} requires more attention as described in the following sections.

B. Input Cost R_{ancs}

The dynamic structure of (17) treats u_{ij} as different inputs for $j = 1 : m(i)$. However, these inputs are generated using one (set of) actuators within the excitation system, and such approach requires a lot of effort from the actuators. To reduce the changes of the inputs between these values and hence minimize the actuator's effort, we propose using an alternative form of R_{ancs} instead of a diagonal matrix that is used for most LQR problems.

$$R_{ancs} \stackrel{\text{def}}{=} \nu \cdot R_D + R_u \qquad (30)$$

R_u is the cost on size of inputs similar to the nominal mode (i.e. LQR with zero delay, with a different size), and ν is the weight on R_D, which is the weight on the differences between segments of each input to minimize chattering of the inputs within each sampling interval.

The weighting on the input R_{ancs} has two parts: i) R_D weight on deviations of the input within each sampling time, and ii) R_u, which is the weight on the size of inputs.

In order to minimize deviations of the input within each sampling time with minimum number of parameters, we define a block diagonal matrix of the following form:

$$R_D = \text{diag}(\rho_1, \rho_2, \cdots, \rho_m), \qquad (31)$$

and define the blocks ρ_i as

$$\rho_i \stackrel{\text{def}}{=} \frac{1}{m(i)} \begin{bmatrix} \rho_i^1 & -1 & \cdots & -1 \\ -1 & \rho_i^2 & \cdots & -1 \\ \vdots & & \ddots & \vdots \\ -1 & -1 & \cdots & \rho_i^{m(i)} \end{bmatrix} \tag{32}$$

where $\rho_i^j = m(i) - 1$, and $m(i)$ is the number of distinct delays (inputs) used in generator i.

The second part includes scaling of R_u, where we choose a diagonal matrix with elements $(r_1, \cdots, r_n)$. Suppose we start with an LQR design for R_u, and scale it with a weight σ.

Remark 1: ρ_i should be chosen such that matrix R_{ancs} is positive definite. Conditions in the form of $\rho_i^j \geq m(i) - 1$ and $R_u \succ 0$ satisfy this requirement.

We investigate the LQR design by fixing the nominal (no delay) LQR weights on states Q_{lqr}, and scaling R_u based on the size of delays τ_{11}, τ_{12}, and τ_{13}. Then we use νR_D to minimize deviations of the inputs within each sampling interval. Therefore, the cost function $\mathscr{J}$ can be written as

$$\mathscr{J} = J_{lqr} + \rho J_D \tag{33}$$

where $J_D \stackrel{\text{def}}{=} \nu U^T[k] R_D U^T[k]$.

C. Effect of Time Delays

In this section, we investigate the effect of delays on control performance. Traditional control design without taking delays into design associate increasing delays with performance degradation of dynamical systems; however, using the delays in the control design may result in a shift in the desired delays.

First we note that time delays have significant effect on the control design as they change matrices of (18). We also note that increasing allowable delays can result in significant reduction in the implementation and maintenance costs. Therefore, we propose a numeral analysis based on the power system model to find a delay combination that result in both desired performance and minimum implementation cost/resource utilization. The overall performance of the controller and the platform is then quantified by a $J_{overall} = \rho_1 \mathscr{J} + \rho_2 \mathscr{J}_I$, where $\mathscr{J}$ is the control performance cost defined in (25), $\mathscr{J}_I$ is the implementation cost, and $\rho_1, \rho_2 \in \mathbb{R}$ are constant parameters. $\mathscr{J}_I$ is chosen so as to reflect the overall average resource utilization and implementation cost of the application. The goal of the co-design algorithm is to find the optimal parameters τ_{ij} that minimize a cost $J_{overall}$.

VI. Wide-Area Control with Delay Overrun

The discussions in the above section imply that as long as $\tau_{wc} < h$, a control design can be carried out as in (23) for the plant in (22), where $\tau = \tau_{wc}$. The platform resources therefore have to be such that τ_{wc} computed using (15) does not exceed h. Any time-variations in τ between $(0, \tau_{wc})$ can be accommodated by using a shaper. By locating the shaper at the last *PE* and having it hold every fully processed sample for exactly $\tau_{th} - \tau$ time units before sending to the actuator, we can ensure that the total end-to-end delay encountered by every PMU data sample from the PMU to the control actuator is always τ_{th}. However, the messages can be dropped or their delays can become too large to be deemed useful. We therefore address in this section the possibility that τ varies, and allow some of the messages to be overrun, i.e. $\tau < \tau_{th}$ for some messages, and $\tau > \tau_{th}$ for others. In this framework, we assume that a single parameter τ_{th} is available, similar in the nominal case described in §IV-B. We allow the possibility for the actual delay τ to vary with respect to τ_{th}. Therefore, we consider the possibility of two cases, described below:

A1. Nominal: $\tau \leq \tau_{th}$, That is, the message has a delay less than the threshold.

A2. Overrun, $\tau > \tau_{th}$: The message suffers a delay greater than τ_{th}. In this case, we propose an abort strategy, where the computation of the current control input is aborted.

We present the details of control design in cases A1 and A2 discussed below. First we present the design for a case with a single delay in the system in §VI-A and then in §VI-B extend the design for WAC with multiple delays from different areas.

A. Abort Strategy for a Single Delay

In this case $\tau > \tau_{th}$. As this implies that the control message $U[k]$ will arrive too close to the end of the interval, computation of $U[k]$ is aborted and $U[k]$ is set to the previously computed value. That is at any time k, the delay τ continues to be larger than τ_{th} for j consecutive instants, with $\tau \leq \tau_{th}$ at $k-1$, then it follows that

$$U[k+\ell] = U^*[k-1], \qquad \ell = 0 : j-1. \tag{34}$$

where $U^*[k-1]$ is a previously computed value. That is, the signal has j drops during which no new control input is computed, but rather an old input is used.

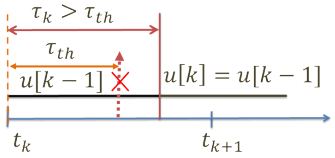

Fig. 3: Abort Strategy, $\tau_k > \tau_{th}$, with a ZOH-based Control Input.

We now present two different control designs with the abort strategy. The first is based on a standard Zero-Order Hold (ZOH), where the previous input in the system is retained as the current input and discussed in §VI-A.1 (illustrated in Figure 3), and the second is a control design based on the number of consecutive drops, denoted as Drop Compensation Control and discussed in §VI-A.2.

1) Case (i): Abort with Zero Order Hold

Let there be i nominal cases followed by j messages for all of which the delays exceed τ_{th}, that is

$$\begin{cases} \tau \leq \tau_{th} & \text{for} \quad k_1 < k \leq k_1 + i & \text{(35a)} \\ \tau > \tau_{th} & \text{for} \quad k_1 + i + 1 \leq k \leq k_1 + i + j. & \text{(35b)} \end{cases}$$

Then the corresponding control input based on zero-order hold is given by

$$U[k] = \begin{cases} K_0 X[k] + G_0 U[k-1] & \text{for } k_1 \le k < k_1 + i \quad (36a) \\ U[k_1 + i] & \text{for } k_1 + i + 1 \le k \le k_1 + i + j. \quad (36b) \end{cases}$$

The reason for the choice of the ZOH-controller as in (36a) and (36b) is self-evident: For $[k_1, k_1 + i]$, the system has a delay less than τ_{th} and as such, the nominal controller proposed in §IV-B is chosen in (36a). Since for $[k_1 + i, k_1 + i + j]$, the message is dropped, the controller is simply set to the previous value in (36b). The question that remains to be addressed is the stability of the closed-loop system for the power system model in (22) and the wide area controller as in (36).

Suppose $j = 1$ in (36). It follows from the discussions in §IV-B that for $k = k_1 : k_1 + i_1$, the power system models is given by

$$X[k+1] = AX[k] + BU[k-1], \quad (37)$$

where $B \stackrel{\text{def}}{=} B_{11} + B_{12}$. A control design as in (23) can then be used over this interval, leading to closed-loop dynamics given by

$$Z[k+1] = \Gamma_n Z[k], \text{ for } k = k_1 : k_1 + i_1, \quad (38)$$

with Γ_n defined as in (24). Since at $k = k_1 + i_1$, there is one drop, it follows that for $k = k_1 + i_1 : k_1 + i_1 + j$,

$$U[k] = U[k-1]. \quad (39)$$

And since at $k_1 + i_1 - 1$, the system is in nominal mode, it follows that

$$U[k-1] = K_0 x[k-1] + G_0 U[k-2]. \quad (40)$$

Therefore, the closed-loop dynamics can be derived by combining (37), (39), and (40) as

$$Z[k+1] = \begin{bmatrix} A & B \\ 0 & I \end{bmatrix} Z[k] \stackrel{\text{def}}{=} \Gamma_a Z[k] \text{ for } k = k_1 + i_1. \quad (41)$$

Therefore, if starting at k_1, there are j_1 drops followed by i_1 instants of the nominal case, it follows that

$$\begin{cases} Z[k_1 + j] = \Gamma_a^j Z[k_1], & j = 1, \cdots, j_1 \\ Z[k_1 + j + i] = \Gamma_n^i Z[k_1 + j_1], & i = 1, \cdots, i_1 \end{cases}$$

In summary, suppose that starting at k, the signal was dropped for the next j_ℓ instants, and i_ℓ instants where it was not dropped, for $\ell = 1 : p$, over $N_a = \sum_{\ell=1}^{p} (i_\ell + j_\ell)$ samples. Let m_a and n_a be defined as

$$m_a \stackrel{\text{def}}{=} \sum_{\ell=1}^{p} j_\ell \qquad n_a \stackrel{\text{def}}{=} \sum_{\ell=1}^{p} (i_\ell). \quad (42)$$

where m_a is the total number of drops over an interval N_a and n_a is the total number of nominals. Then the evolution of the switched system over a time window $[k_1, k_1 + N_a]$, $N_a = m_a + n_a$, is given by

$$Z[k + N_a] = \Gamma_n^{i_p} \Gamma_a^{j_p} \cdots \Gamma_n^{i_2} \Gamma_a^{j_2} \Gamma_n^{i_1} \Gamma_a^{j_1} Z[k] \quad (43)$$

Remark 2: We note that in (43), over any interval $[k, k + N_a]$, the sequence $j_1, i_1, \cdots, j_p, i_p$ can vary, with p varying as well, with the only constraint that $m_a \le m_{a0}$ and the i's such that $n_a = N_a - m_a \ge n_{a0}$, where m_{a0} and n_{a0} are fixed upper and lower bounds on the drops and nominals, respectively. We discuss conditions under which the switching dynamics in (43) is stable in Theorem 1. In what follows,

$$\begin{bmatrix} A & * \\ B & D \end{bmatrix} \stackrel{\text{def}}{=} \begin{bmatrix} A & B^T \\ B & D \end{bmatrix} \quad (44)$$

Theorem 1: System (43) is stable (exponentially stable) if there exist positive definite matrix $P \succ 0$, and positive scalars $\gamma_1, \gamma_2 > 0$ such that the following Linear Matrix Inequalities (LMI) are satisfied:

$$\begin{bmatrix} -\gamma_1 P & * \\ P\Gamma_n & -P \end{bmatrix} \prec \mathbf{0}, \quad (45)$$

$$\begin{bmatrix} -\gamma_2 P & * \\ P\Gamma_a & -P \end{bmatrix} \prec \mathbf{0}, \quad (46)$$

with

$$\gamma_1^{n_{a0}} \cdot \gamma_2^{m_{a0}} \stackrel{\text{def}}{=} \alpha_a^{-2} \le 1 (< 1). \quad (47)$$

where $\alpha_a > 1$ is the exponential decay rate over interval of N_a samples.

Proof: See Appendix I. ■

2) Case (ii): Drop Compensation Strategy

The second method is based on a control action that varies explicitly with the number of drops. For the abort case as described in (35), for any $k \ge k_1 + i + 1$, the drop compensation control is chosen to be of the form

$$U[k + \ell] = K_\ell X[k-1] + G_\ell U[k + \ell - 1], \qquad \ell = 0 : j - 1. \quad (48)$$

That is, for the case when there are j PMU data drops starting $k_1 + i + 1$ following i nominals, the control input is computed using previous measurements, and K_ℓ,G_ℓ are gains that are precomputed depending on the number of drops ℓ. In what follows, we show how these gains can be computed so as to guarantee closed-loop stability. For the abort case as in (35), the drop compensation controller has the structure

$$U[k] = \begin{cases} K_0 X[k_1] + G_0 U[k_1 - 1] & \text{for } k_1 \le k < k_1 + i \stackrel{\text{def}}{=} k_2 \quad (49a) \\ K_\ell X[k_1 + i] + G_\ell U[k_1 + i - 1] & \text{for } k_2 + 1 \le k \le k_2 + j, \ell = 1 : j. \quad (49b) \end{cases}$$

The closed-loop system with the plant as in (22) and the control as in (49) can now be derived. If (49a) is used, the closed-loop system dynamics is given by (24). Proposition 1 describes the closed-loop dynamics when (49b) is used.

Proposition 1: For the power system model in (22) and the control input given in (49) for the abort case given in (35), the closed-loop dynamics is of the form

$$Z[k+1] = \begin{bmatrix} A_K & A_G \\ K_i & G_i \end{bmatrix} Z[k-j] \stackrel{\text{def}}{=} A_m^{(j)} Z[k-j], \quad (50)$$

where

$$A_K \stackrel{\text{def}}{=} A^{j+1} + \sum_{\ell=1}^{j} A^{j-\ell} A_B K_{\ell-1} + B_{11} K_j$$

$$A_G \stackrel{\text{def}}{=} A^j B_{12} + \sum_{\ell=1}^{j-1} A^{j-\ell} A_B G_{\ell-1} + B_{11} G_j$$

Proof: See Appendix II. ∎

The stability of the overall closed-loop system for the abort case in (35), with the drop compensation control as in (49) is now summarized in Theorem 2.

Theorem 2: K_i and G_i, $i = 1 : m_a$ exist such that (43) is stable(exponentially stable) if there exist positive definite matrices $Q_i \succ 0$, and positive scalars $\gamma_i > 0$ such that the following LMI are satisfied for some matrices E_i and F_i:

$$\begin{bmatrix} -\gamma_0 Q_1 & \mathbf{0} & * & * \\ \mathbf{0} & -\gamma_0 Q_2 & * & * \\ AQ_1 + B_{11}E_0 & B_{12} + B_{11}F_0 & -Q_1 & 0 \\ E_0 & F_0 & \mathbf{0} & -Q_2 \end{bmatrix} \prec \mathbf{0}, \quad (51)$$

$$\begin{bmatrix} -\gamma_j Q & * \\ \mathscr{L}_j & -\gamma_j Q \end{bmatrix} \prec \mathbf{0}, \;\; j = 1 : m \quad (52)$$

where

$$Q \stackrel{\text{def}}{=} \begin{bmatrix} Q_1 & 0 \\ 0 & Q_2 \end{bmatrix},$$

$$\mathscr{L}_j \stackrel{\text{def}}{=} \begin{bmatrix} A^{j+1}Q_1 + \sum_{\ell=1}^{j} A^{j-\ell}A_B E_{\ell-1} + B_{11}E_j & A^i B_2 Q_2 + \sum_{\ell=1}^{j-1} A^{j-\ell}A_B F_{\ell-1} + B_{11}F_j \\ E_j & F_j \end{bmatrix}$$

and

$$K_i = E_i Q_1^{-1} \;\; G_i = F_i Q_2^{-1}, \;\; \max(\gamma_0^n \cdot \gamma_i^m) \stackrel{\text{def}}{=} \alpha_{DCC}^{-2} \leq 1 (< 1). \quad (53)$$

where $\alpha_{DCC} > 1$ is the least exponential decay rate over $m_a + n_a$ samples.

Proof: See Appendix III. ∎

Remark 3: Although Theorem 2 results in guaranteed performance for the system with dropped signals, it may result in infeasibility of LMI. An alternative approach is to design the controllers for the dropped modes and evaluate robustness of the system to the worst combination of the drops with an approach similar to [10].

B. Abort Strategy with Multiple Delays

In a practical wide-area network, any arbitrary PMU data sample can be dropped while transmission using TCP or UDP protocols. Therefore, instead of dealing with all delays as a single delay, we should consider presence of multiple messages in the system. This can be done by expanding the number of LMI in Theorem 1 and Theorem 2. First we notice that instead of a single matrix Γ_a for the abort mode, there are several matrices Γ_{a_i} depending on the combination of possible drops. For example, if drops can happen only for inter-area messages, n_τ, the number of matrices Γ_{a_i} that should be considered in the analysis or the design of this system includes single drops and a combination of multiple drops at the same time. Γ_{a_i} can be found by setting $u_{ij}[k]$ to $u_{ij}^*[k]$ of the respective message in (17). Now, we present the following corollaries for multiple delays.

Corollary 3: System (43) is stable (exponentially stable) if there exist positive definite matrix $P \succ 0$, and positive scalars $\gamma_1, \gamma_2 > 0$ such that the following Linear Matrix Inequalities (LMI) are satisfied:

$$\begin{bmatrix} -\gamma_1 P & * \\ P\Gamma_n & -P \end{bmatrix} \prec \mathbf{0}, \quad (54)$$

$$\begin{bmatrix} -\gamma_2 P & * \\ P\Gamma_{a_i} & -P \end{bmatrix} \prec \mathbf{0}, \forall i = 1 : n \quad (55)$$

with

$$\gamma_1^{n_{a0}} \cdot \gamma_2^{m_{a0}} \stackrel{\text{def}}{=} \alpha_a^{-2} \leq 1 (< 1). \quad (56)$$

where $\alpha_a > 1$ is the exponential decay rate over interval of N_a samples, and n_τ is the number of different modes that should be considered depending on the possibility of aborting messages.

VII. Case Study on a 50-bus Australian Power System Model

In this section, we illustrate our proposed design method using a power system model with 50 buses and 14 generators, as shown in Fig. 1(a) [15]. The network is divided into four areas. The generators in each area, denoted by red dots, are: $G_1 - G_5$ in Area 1, $G_6 - G_7$ in Area 2, $G_8 - G_{11}$ in Area 3, and $G_{12} - G_{14}$ in Area 4. In order to evaluate the robustness of this system to the delays, we consider three sets of delays for local, intra-area, and inter-area communications as discussed in §IV. We assume that the local delays are negligible $\tau_{ii} \approx 0$, whereas the intra-area delays that are the results of communications through dedicated subnetwork channels inside each area are $\tau_{ij} = 30$ ms, and the inter-area communication delays via the Internet are about 60 ms. In what follows, we discuss the results of the proposed optimal controller, and compare the delay-aware controller to an optimal controller without delay in the design. An example of performance optimization based on the combinations of local, intra-area, and inter-area delays is given in §VII-B. An analysis of possible dropped signals and the performance of the system subject to aborted signals are presented in §VII-C.

A. Optimal Control with No Overrun

We first design an LQR excitation controller ΔE_F for (8) assuming that the feedback from the PMUs is instantaneous, i.e., there is no network delay. The closed-loop phase angle response of G_1, as shown by the blue curve in Fig. 4, is observed to be satisfactorily damped. However, when we implement this LQR controller in presence of network delays, the closed-loop system loses stability as shown by the red curve in the figure. This clearly indicates how any excitation controller which is completely negligent of delays may end up destabilizing the grid during a disturbance. To circumvent this instability, we design our delay-aware ANCS controller and re-stabilize the system as testified by the magenta curve in Fig. 4. For this particular system the ANCS controller, in fact, almost recovers the nominal closed-loop response. The corresponding control inputs for these three designs are shown in Fig. 5. Again, it must be observed that the input signal diverges sharply if the controller is oblivious to the delays. The ANCS controller, although slightly more chattering than the nominal controller, recovers closed-loop stability, and for this example closed-loop performance as well.

Figures 6(a) and 6(b) respectively show the phase angle and velocity responses for all 14 generators. It can be seen that all states remain bounded within a small neighborhood of the initial equilibrium. The rate of convergence of these

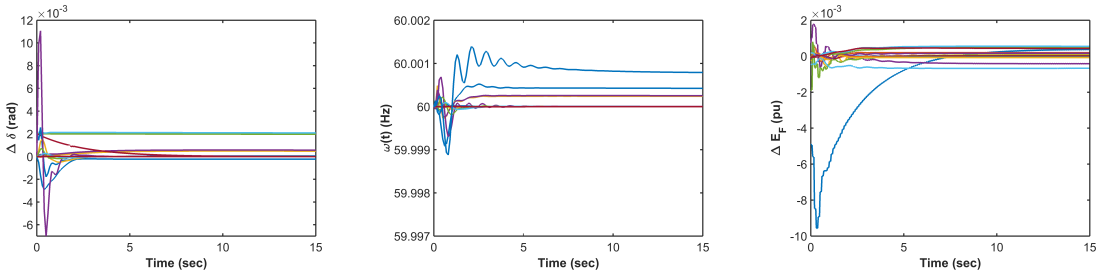

(a) Phase angle deviations of all generators (b) Rotor velocities of all generators (c) Excitation input to the generators

Fig. 6: Evaluation of the ANCS Design with: local delays= 0, intra-area delays= 30ms , and inter-area delays= 60

states can be controlled by appropriately tuning the constants α_{ij} and β_j as in (29). Figure 6(c) shows the arbitrated control inputs for the 14 generators. Depending on the choice of R_n the input can exhibit chattering. This is one drawback of this design, but if needed it can be avoided by placing a saturation block on the amplitude of the excitation voltage.

B. *Effect of Delay Combinations on control Design and Performance*

Figure 7 shows a plot of In order to find the combination of delays, a combination of delays are investigated to determine

While in conventional control design, increasing time delays are usually associated with decreasing performance of the systems. We showed that when delays are taken in the control design, increasing delays from zero can result in better control performance.

C. *Message Dropout Analysis*

In this section, we used the same LQR controller as the previous section in combination with a zero-order hold block. Therefore, results ofn we used Theorem 1 to find the maximum drop rates for the controller. For the result of this section, we assumed that only the inter-area messages can be dropped. A norm-based approach was used to estimate the maximum rate of drops that the system can tolerate without becoming unstable. the analysis showed that the ancs system can tolerate up to 30% drop rate from the inter-area messages. however, the quality of control degrades and the system response slower.

Figure 8 shows the network traffic for the six inter-area communication links connecting the VPN routers of the four areas, as shown in Figure 1b. We assume all-to-all connection between the routers. The N state means that a link has normal SDN traffic, and therefore, can pass data packets successfully from PMUs to controllers. The C state, however, means that the link encounters a congestion status due to heavy instantaneous traffic in the SDN, and thereby fails to deliver the data packet, which is then treated as dropped. Once the status goes back to N, the link can transfer packets again, without dropping them. The corresponding closed-loop response of the frequency of G_1 with abort strategy is shown in Figure 9(a) compares input of the system when there are no aborted signals versus the case that 30% of inter-area messages drop. Figure 9(b) shows a comparison of the output of the system. these figures prove the stability of the system, while degradation of the control performance when the drops happen frequently.

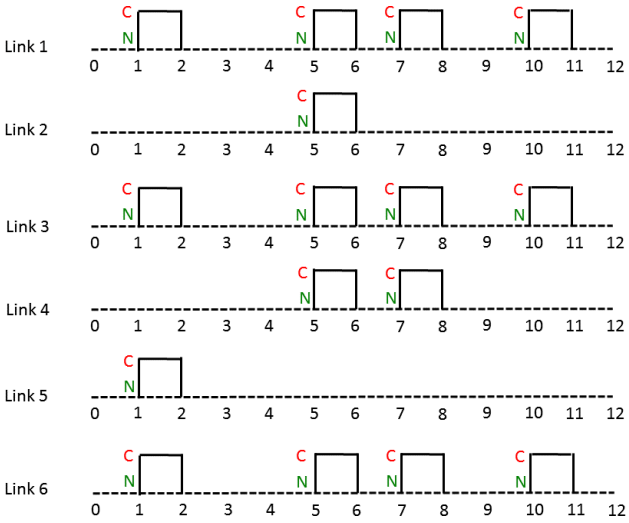

Fig. 8: Timing diagram showing possible drops in the system with C representing congestion and N representing normal

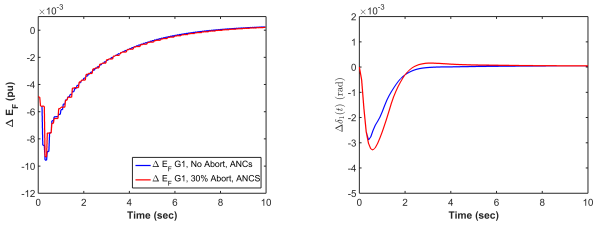

(a) Phase Angle of G_1 (b) Inputs of G_1

Fig. 9: Effect of 30% abort on control performance

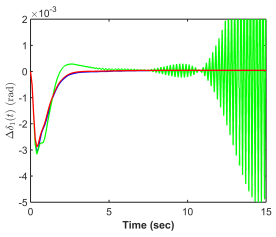

Fig. 4: Phase Angle of G_1

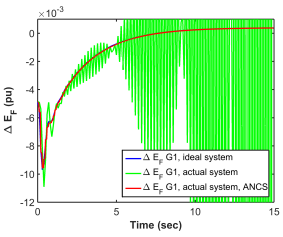

Fig. 5: Inputs of G_1

VIII. Conclusions

In this paper we presented an arbitrated network control design for wide-area optimal control of power systems using Synchrophasors in presence of communication delays. We showed that our control design depends on the estimates of the worst-case delay, and that by regulating the delay in the control messages appropriately it is possible to guaran-

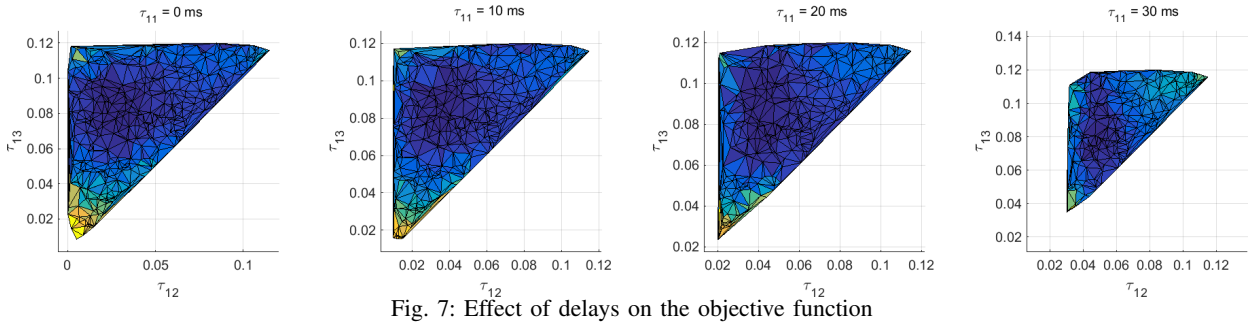

Fig. 7: Effect of delays on the objective function

tee both stability and optimal performance of the closed-loop system. Our simulations illustrate that this approach is superior to traditional robust controllers, especially for combating variable delays that are commonly found in wide-area communication networks.

REFERENCES

[1] A. G. Phadke and J. S. Thorp, *Synchronized phasor measurements and their applications*. Springer Science & Business Media, 2008.

[2] A. Chakrabortty and P. Khargonekar, "Introduction to wide-area control of power systems," in *ACC'13*, June 2013, pp. 6758–6770.

[3] D. Reiners, "Opensg: A scene graph system for flexible and efficient realtime rendering for virtual and augmented reality applications," Ph.D. dissertation, Reiners, Dirk, 2002.

[4] S.-Y. Wang, C.-L. Chou, and C.-M. Yang, "Estinet openflow network simulator and emulator," *IEEE Communications Magazine*, vol. 51, no. 9, pp. 110–117, 2013.

[5] R. Hasan, R. Bobba, and H. Khurana, "Analyzing NASPInet data flows," in *PSCE'09*. IEEE, 2009, pp. 1–6.

[6] P. Myrda, J. Taft, and P. Donner, "Recommended approach to a naspinet architecture," in *45th Hawaii International Conference on System Science (HICSS)*, Jan 2012, pp. 2072–2081.

[7] H. Wu, H. Ni, and G. Heydt, "The impact of time delay on robust control design in power systems," in *IEEE Power Engineering Society Winter Meeting*, vol. 2, 2002, pp. 1511–1516 vol.2.

[8] G. Taranto, J. Chow, and H. Othman, "Robust redesign of power system damping controllers," *IEEE Trans. Control Syst. Technol.*, vol. 3, no. 3, pp. 290–298, Sep 1995.

[9] A. M. Annaswamy, D. Soudbakhsh, R. Schneider, D. Goswami, and S. Chakraborty, "Arbitrated network control systems: A co-design of control and platform for cyber-physical systems," in *Control of Cyber-Physical Systems*. Springer, 2013, pp. 339–356.

[10] D. Soudbakhsh, L. Phan, O. Sokolsky, I. Lee, and A. Annaswamy, "Co-design of control and platform with dropped signals," in *IC-CPS'13*, April 2013.

[11] D. Soudbakhsh, L. Phan, O. Sokolsky, and A. Annaswamy, "Co-design of arbitrated network control systems with overrun strategies," *Submitted to the IEEE Trans. Control of Network Systems*, 2015.

[12] P. M. Anderson and A. A. Fouad, *Power system control and stability*. John Wiley & Sons, 2008.

[13] F. Dorfler, M. R. Jovanovic, M. Chertkov, and F. Bullo, "Sparse and optimal wide-area damping control in power networks," in *ACC'13*, 2013, pp. 4289–4294.

[14] G. Hooghiemstra and P. Van Mieghem, "Delay distributions on fixed internet paths," Delft University of Technology, Tech. Rep., 2001.

[15] M. Gibbard and D. Vowles, "Simplified 14-generator model of the se australian power system," *The University of Adelaide, Australia*, 2008.

APPENDIX I
PROOF OF THEOREM 1

Proof: Inequality (54) implies that the following inequalities are satisfied as well, with the Schur complement:

$$\Gamma_n^T P \Gamma_n \prec \gamma_1 P, \tag{57}$$

similarly, we can show that inequality (55) implies that

$$\Gamma_m^T P \Gamma_m \prec \gamma_2 P, \tag{58}$$

Also, we note from (43) that starting at time k_1, there are at least n_{a0} nominal signals and at most m_{a0} dropped signals; with $\gamma_2 \geq 1 > \gamma_1 \geq 0$ we have:

$$\left(\Gamma_n^{i_p}\Gamma_m^{j_p}\cdots\Gamma_n^{i_2}\Gamma_m^{j_2}\Gamma_n^{i_1}\Gamma_m^{j_1}\right)^T P \left(\Gamma_n^{i_p}\Gamma_m^{j_p}\cdots\Gamma_n^{i_2}\Gamma_m^{j_2}\Gamma_n^{i_1}\Gamma_m^{j_1}\right) < \gamma_1^n\gamma_2^m P < \alpha^{-2}P \tag{59}$$

with $\alpha^{-2} \stackrel{\text{def}}{=} \gamma_1^{n_{a0}}\gamma_2^{m_{a0}}$.

These inequalities imply that a quadratic Lyapunov function in the form of $V = X[k]^T P X[k]$ exists for systems (54) and (55), and it is decreasing with a decay rate of at least α for any interval $N_a = m_a + n_a$, proving Theorem 1. ■

APPENDIX II
PROOF OF PROPOSITION 1

Proof: If (49a) is used, the closed-loop system corresponds to (48). If (49b) is used, the closed-loop system should be written in the same form as (48) to allow for a switching design as is derived below.

Suppose the drops occur starting at $k = k_1 + i_1$. If $j = 1$ in (49b), then

$$x[k+1] = Ax[k] + B_{11}u_d[k] + B_{12}u[k-1], \tag{60}$$

where $u_d[k]$ is the current input that is computed using old available information. Noting that the previous signal was a nominal one, from (48) and (49a) we have

$$\begin{aligned} x[k] &= Ax[k-1] + B_{11}u[k-1] + B_{12}u[k-2] \\ u[k-1] &= K_0x[k-1] + G_0u[k-2] \end{aligned} \tag{61}$$

Using (61) and (60) we write (60) as

$$\begin{aligned} x[k+1] = {} & (A^2 + AB_{11}K_0 + B_{12}K_0)x[k-1] + \\ & (AB_{11}G_0 + B_{12}G_0)u[k-2] + B_{11}u_d[k]. \end{aligned} \tag{62}$$

Based on (62), we design a controller in the form of (49b) to stabilize the plant in the drop mode. Therefore, with $X[k] = [x[k]^T, u[k-1]^T]^T$, the closed-loop dynamics in the drop mode becomes

$$X[k+1] = \begin{bmatrix} AA_{K1} & A_{G1} \\ K_1 & G_1 \end{bmatrix} X[k-1] \stackrel{\text{def}}{=} A_m^{(1)} X[k-1]. \tag{63}$$

where $A_{K1} \stackrel{\text{def}}{=} A^2 + (AB_{11} + B_{12})K_0 + B_{11}K_1$ and $A_{G1} \stackrel{\text{def}}{=} (AB_{11} + B_{12})G_0 + B_{11}G_1$. For a general j number of drops, we have that

$$u_d[k] = K_i x[k-j] + G_i u[k-j-1].$$

which results in the following form for the closed loop dynamics of the system with j consecutive drops and the control strategy (60):

$$X[k+1] = \begin{bmatrix} A_{Kj} & A_{Gj} \\ K_i & G_i \end{bmatrix} X[k-j] \stackrel{\text{def}}{=} A_m^{(j)} X[k-j], \tag{64}$$

where

$$A_{Kj} \stackrel{\text{def}}{=} A^{j+1} + \sum_{\ell=1}^{j} A^{j-\ell}(AB_{11} + B_{12})K_{\ell-1} + B_{11}K_j \tag{65}$$

$$A_{Gj} \stackrel{\text{def}}{=} A^j B_{12} + \sum_{\ell=1}^{j-1} A^{j-\ell} A_B G_{\ell-1} + B_{11}G_j \tag{66}$$

■

APPENDIX III
PROOF OF THEOREM 2

Proof: Proof of Theorem 2 follows the same procedure as the proof of Theorem 1 as stated in Appendix I, using Proposition 1. ■